

1-1-2018

Transfer of the protonable surfactant dipalmitoyl-phosphatidylcholine across a large liquid/liquid interface: a voltammetric study

İBRAHİM UYANIK

Follow this and additional works at: <https://journals.tubitak.gov.tr/chem>

 Part of the [Chemistry Commons](#)

Recommended Citation

UYANIK, İBRAHİM (2018) "Transfer of the protonable surfactant dipalmitoyl-phosphatidylcholine across a large liquid/liquid interface: a voltammetric study," *Turkish Journal of Chemistry*. Vol. 42: No. 2, Article 6. <https://doi.org/10.3906/kim-1701-6>

Available at: <https://journals.tubitak.gov.tr/chem/vol42/iss2/6>

This Article is brought to you for free and open access by TÜBİTAK Academic Journals. It has been accepted for inclusion in Turkish Journal of Chemistry by an authorized editor of TÜBİTAK Academic Journals. For more information, please contact academic.publications@tubitak.gov.tr.

Transfer of the protonable surfactant dipalmitoyl-phosphatidylcholine across a large liquid/liquid interface: a voltammetric study

İbrahim UYANIK*

Department of Metallurgical and Materials Engineering, Faculty of Technology, Selçuk University, Konya, Turkey

Received: 02.01.2017

Accepted/Published Online: 14.09.2017

Final Version: 27.04.2018

Abstract: Adsorption behavior of the zwitterionic phospholipid dipalmitoyl-phosphatidylcholine (DPPC) at the polarizable liquid/liquid interface formed between water and 1,2-dichloroethane electrolyte solutions is studied taking into account both the pH of the aqueous phase and the concentration of the phospholipid in the organic phase by cyclic voltammetry. Experimental results showed that the adsorption of the phospholipid strongly depends on the pH of the aqueous phase, which determines the surface ionization of the polar head of the phospholipid molecule and hence the stability of the adsorbed layer of phospholipids.

Key words: Interface between two immiscible electrolyte solutions, adsorption, facilitated proton transfer, ion transfer voltammetry

1. Introduction

A liquid/liquid interface is formed between two solvents of low mutual miscibility. One of these solvents is water (W) and the other one is a polar organic solvent with a relatively high dielectric permittivity, such as nitrobenzene or 1,2-dichloroethane (DCE). The liquid/liquid interface can also be either polarizable or nonpolarizable, depending on permeability to charged species distributed in either or both phases.^{1–4} The liquid/liquid interface has long been recognized as a very simple model system to mimic biomembranes. Indeed, adsorbed monolayers of phospholipids can be used to simulate half a biological membrane. The advantage of the liquid/liquid interface approach compared to black lipid membranes supported either at the tip of a micropipette or on a microhole in a thin Teflon wall is that the potential distribution across the interface can be easily controlled, and that the surface pressure of the monolayer can be monitored.^{5–9}

Many publications have been dedicated to the characterization of the physical properties of adsorbed monolayers at the interface between two immiscible electrolyte solutions (ITIES). The adsorption of phosphatidylethanolamine (PE) and phosphatidylcholine (PC) at an ITIES can be modulated by varying either the externally applied potential or the pH of the aqueous phase.^{10,11} Thus, interfacial tension measurements as a function of the potential difference between the two phases, called electrocapillary measurements, have been used to characterize the adsorbed monolayer. This methodology has been extended over the last decade to study the interactions of neutral and/or charged species with phospholipids and to determine the Gibbs energy of interaction. The electrocapillary curves have also been interpreted to explain in detail their behavior. More importantly, this electrochemical methodology has shown for the first time that phospholipids can act

*Correspondence: iuyanik@selcuk.edu.tr

as ionophores to complex hydrophilic ions and allow their extraction to the organic phase.¹² The onset of the interfacial tension increase is dependent on the pH as well as on the presence of other species in the aqueous phase. These electrocapillary curves clearly show that PCs are capable of forming complexes with a wide variety of cations in addition to the proton, including Na^+ , K^+ , Ca^{2+} , Li^+ , and Arg^+ (arginine).¹³

Until recently, there were very few electrochemical investigations to monitor aqueous ion/phospholipid interactions under controlled polarization.^{14,15} In the literature, the interaction between alkali and alkaline-earth cations with a phospholipid monolayer at the water/DCE interface was also studied.¹⁶ In a very general way, the transfer of these cations across a dibehenoyl-phosphatidylcholine (DBPC) monolayer was analyzed by cyclic voltammetry and capacitance measurements. Cation adsorption processes at the polar head of the phospholipid were identified and, at the same time, after adsorption, an enhancement or a blocking of the transfer process was produced, depending on the nature and concentrations of the probe cation. For example, Li^+ seems to induce a packing effect over the lipidic monolayer, hindering in this way any ion transfer process. However, it has been shown that PCs can act as ionophores to facilitate the transfer of alkali metal ions and it was demonstrated that the phospholipids can complex cations, and that under a given polarization of the interface the complex could be transferred to the organic phase.¹⁷

Considering the strong interaction between the phospholipid polar head and aqueous metallic cations, a five-step mechanism for the formation and behavior of DPPC monolayers at the W/DCE interface in which adsorption and ion-pairing processes are involved has been proposed.^{18–21} Additional results have been obtained at the air/liquid interface by researchers reporting the calcium-induced ordering over monolayers made of either positively or negatively charged phospholipids.²² This specific adsorption/desorption of ions and ion-pairing processes at the ITIES has been proved to greatly alter the current signals observed in common voltammetric experiments^{14,17,23} and interfacial tension measurements.^{10,16,24} The voltammetric responses associated with the combined ion adsorption/ion transfer processes have also been theoretically addressed in the literature.²⁵ More recently, assisted proton transfer by phospholipids across a liquid/liquid interface has been utilized for solar fuel generation.²⁶

In this paper we report our experimental results from a large liquid/liquid interface (W/DCE) by ion transfer voltammetry to confirm the previously proposed mechanisms of facilitated proton transfer to extend them, controlling both the pH of the aqueous phase and the phospholipid concentration in the organic phase.

2. Results and discussion

A representation of the electrochemical cells used for voltammetric measurements is given in Figure 1.

The dashed line in Figure 2 shows the polarization window or polarizable potential window obtained with Cell 1 in Figure 1. There is only a very small amount of current flow within the potential window in response to the applied potential, and this occurred as a result of the interfacial charging current.²⁷ On the other hand, at the outside of the polarizable potential window, the ions of the supporting electrolyte begin to transfer from their original phase to out-of-phase. This condition causes the base electrolyte current (background current) to increase. Because assigning the interface polarization is traditionally done based on an aqueous phase, the right-hand side of the curve in Figure 2 means that the aqueous phase is positive. That is, the aqueous phase becomes more positive towards the right side of the curve.²⁷

As the polarization continues, the TB^- ions in the organic phase start to transfer to the aqueous phase while Cs^+ ions in the aqueous phase transfer from the water to the organic phase. The relative contributions of

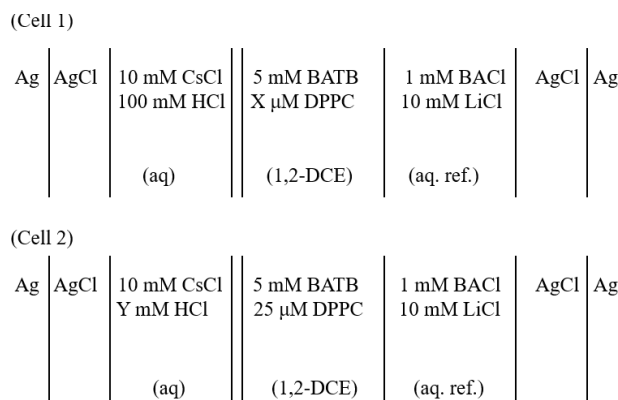


Figure 1. Electrochemical cells employed. The double lines stand for the water/DCE interfaces under consideration (area = 1.53 cm²).

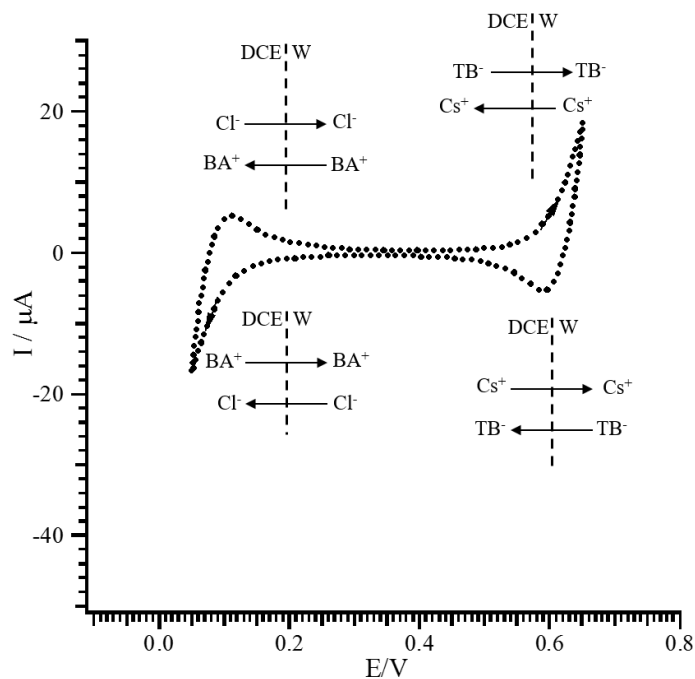


Figure 2. Polarizable potential window measured at the interface composed of Cell 1 of Figure 1 and interfacial processes (scan rate: 50 mV/s, X = 0).

these ions to the current depend on the values of these ions on the scale of Gibbs transfer energies.²⁸ In other words, if transfer of ions requires a lower energy, then the contribution of that ion to the observed background current is greater. Because ions of the supporting electrolyte used here have approximately the same energy values, they have an equal contribution to the background current. When the direction of the potential scan is reversed, the Cs⁺ ions transferred into the organic phase start to transfer into the aqueous phase. Then the TB⁻ ions transferred into the aqueous phase start to transfer into the organic phase again. The current results from charging the interface as the potential scanning continues towards the left side at the polarization window. Accordingly, the aqueous phase becomes less positive compared to the organic phase. Therefore, BA⁺ ions in the organic phase start to transfer into the aqueous phase while Cl⁻ ions in the aqueous phase transfer into the

organic phase. When the potential scanning is reversed, the Cl^- ions transferred into the organic phase start to transfer into the aqueous phase, and BA^+ ions transferred into the aqueous phase transfer into the organic phase again. The result showed that about 0.7 V of the potential interval for electrochemical reactions can be studied with these supporting electrolytes.

The following voltammograms (Figure 3) were obtained at the W/DCE interface using Cell 1 in Figure 1. The water phase shown in Cell 1 contained 100 mM HCl. All electrochemical peaks were obtained with phospholipid adsorption at the interface consisting of an aqueous phase with HCl and a DCE organic phase. This is because no voltammetric peak within the potential window was obtained regarding the adsorption of phospholipids at the interface consisting of the aqueous phase without HCl and a DCE organic phase. However, adsorption/desorption of phospholipids at the interface could be noticed visually via changes in the interfacial appearance.^{29,30} It is also very important to note that the cyclic voltammograms (CVs) in the presence of the phospholipid were recorded after 60 s of delay at an initial potential to confirm if the phospholipid had a maximum level of adsorption at the interface.

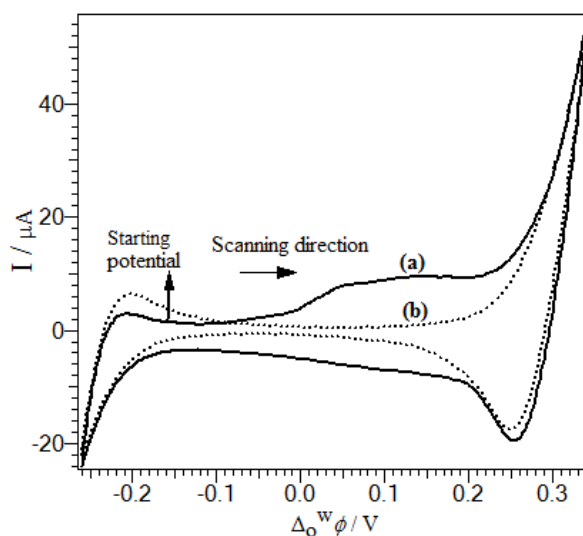


Figure 3. Cyclic voltammograms in the presence (a) and in the absence (b) of 25 μM DPPC by using Cell 1 in Figure 1. Scan rate was 50 mV/s.

The CVs in Figure 3 show that the positive current centered at about 0.15 V is observed at the positive end of the polarizable potential window. This can be explained by adsorption of phospholipids in the organic phase at the interface. This happens first at lower potential values (more negative potentials).¹³ Figure 3 shows that phospholipid molecules adsorbed at the interface start to be desorbed towards the organic phase when the potential scan begins. However, the H^+ ions in the aqueous phase can form a complex with the adsorbed phospholipid molecules at the interface. This situation seems to be compatible with previous models as well.^{13,23} Therefore, the positive current observed from the voltammogram probably results from the desorption of the phospholipid-proton complex, which facilitates the ion transfer of protons into the organic phase. Figure 4 shows the effect of phospholipid concentration on DPPC adsorption at the W/DCE interface. In this figure, all CVs are present on the same current axis to clearly reveal differences in peak heights.

The forward scans of the voltammograms in Figure 4 are corrected by the base electrolyte currents (Figure 5). In this way, we integrated the voltammograms to know the charge or surface concentration of the DPPC

adsorbed at the interface during the forward scans. Charge flow in the system during the forward scan of all CVs (such as between potentials E1 and E2, as shown in Figure 4) were calculated according to literature.³⁷

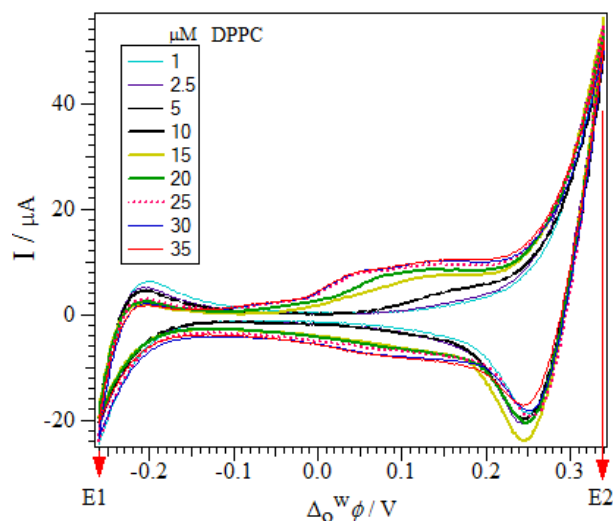


Figure 4. Cyclic voltammograms at the W/DCE interface in the presence of different concentrations of DPPC in DCE phase using Cell 1. Scan rate was 50 mV/s.

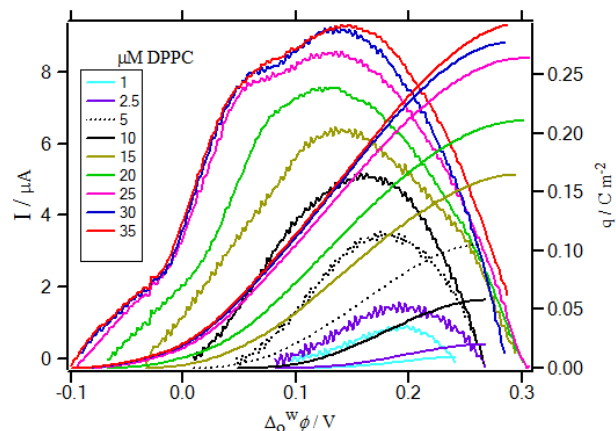


Figure 5. Forward scans of the voltammograms given in Figure 4 corrected for the base electrolyte current and the passed electrical charge q .

On the other hand, in Figure 6a, charge values at the interface are shown as a function of phospholipid concentration in the organic phase. The electrical charge passing through the system is proportional to initial surface concentration of the adsorbed phospholipid assuming that the forward peak currents in the voltammograms resulting from desorption of phospholipids were adsorbed at the interface. These became charged by creating a complex with the proton.^{13,23}

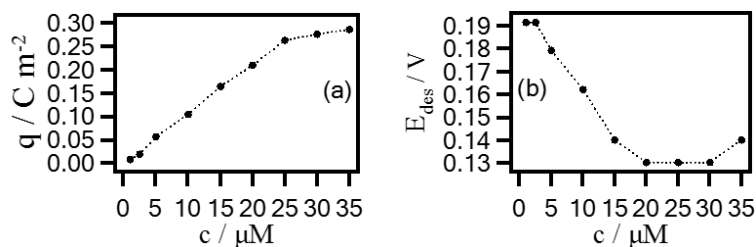


Figure 6. The plot of concentration values of DPPC vs. the electrical charge passed on forward scan (a); desorption potentials of the DPPC (b).

According to the figures, the DPPC concentration in the bulk organic phase no longer affects charge after $\sim 20 \mu\text{M}$. This condition indicates formation of a saturated monolayer with this limit value at the interface. This corresponds to the plateau zone in the graphics.¹³ When Figure 4 is examined again, the potential energy (E_{des}) at which desorption of the complex occurs decreases as a function of the bulk phospholipid concentration in DCE (Figure 6b). Thus, it increases at the interface.

The desorption potential is a potential corresponding to the maximum value of peaks appearing during the voltammetric forward scans.^{18,29} One explanation for the decrease in this potential is that it depends on the phospholipid concentration: increasing the phospholipid concentration in the bulk organic phase means

increasing the number of phospholipid molecules that are adsorbed at interface. Thus, more complexes will form at the interface and desorption will start earlier. This produces the curves seen in Figure 4.

The adsorption of phospholipid has a linear correlation between scan rates and current values. This increases charge flow and results in the peak currents seen in the voltammograms. Figure 7 shows current values obtained with different scan rates.

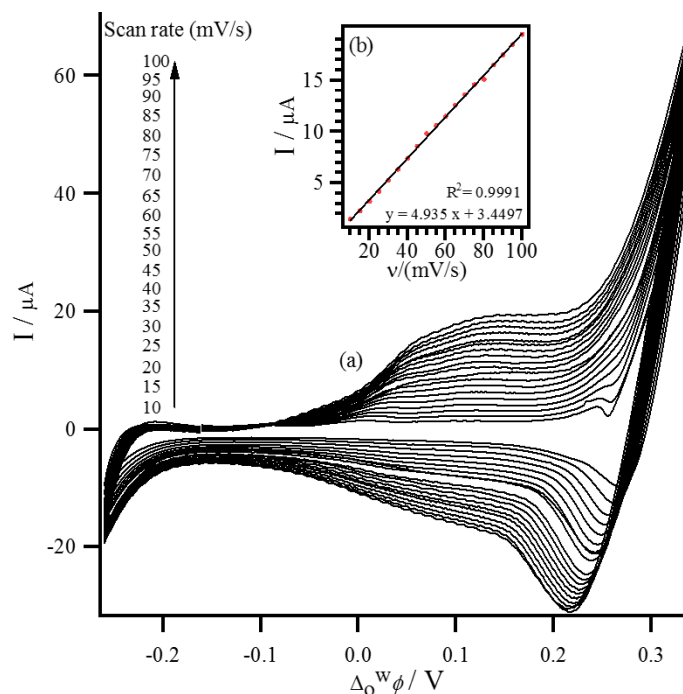


Figure 7. Dependence of peak currents (forward and backward) on scan rates (a). The inset (b) shows a plot of the forward peak currents and scan rates. CVs were recorded at the ITIES in the presence of 25 μM phospholipid with Cell 1.

Figure 7 shows that the heights of the forward peaks are directly proportional to scan rates—this situation is associated with adsorption of DPPC at the interface and thus charging of the electrical double layer.²⁵ When voltammograms are examined, e.g., in Figure 8, the values of forward and backward peak currents are not exactly equal. This difference, of course, varies depending on phospholipid concentrations at the interface. This difference between peak currents might be associated with the difference between adsorbed and desorbed phospholipid concentrations. Namely, some part of the adsorbed phospholipid molecules interacts with the anion of the organic phase and stays there. This result is in agreement with an earlier report in the literature.¹⁸ Therefore, the number of phospholipid molecules affects the change in the current.

To determine the effect of pH on the adsorption of phospholipid, we studied the DCE interface containing 25 μM DPPC with an aqueous phase of variable pH. The forward voltammetric currents facilitate the transfer of protons through the interface via phospholipids. The transfer potential will also have lower values with increasing proton concentration in the bulk aqueous solution. Figure 9 shows CVs obtained from the interface formed between aqueous solutions of different pH values and DCE containing 25 μM DPPC using Cell 2 of Figure 1.

The increase in phospholipid concentration also explains the increasing H^+ ion concentration in the aqueous phase. Thus, DPPC desorbs at higher potential values as aqueous pH increases (Figure 10a). In

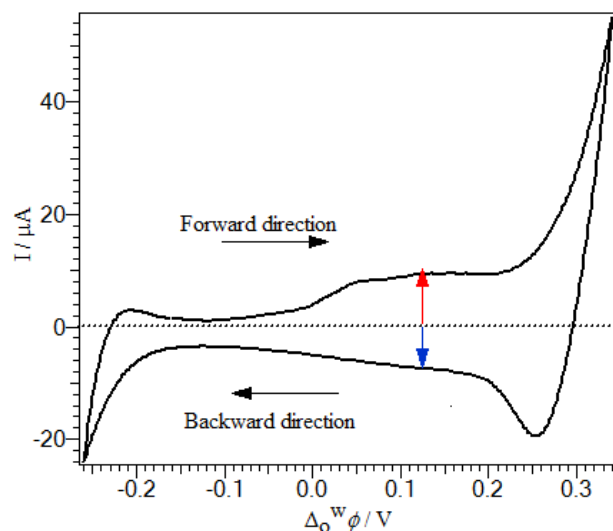


Figure 8. Cyclic voltammogram in the presence of 25 μM DPPC by using Cell 1 in Figure 1. Scan rate was 50 mV/s.

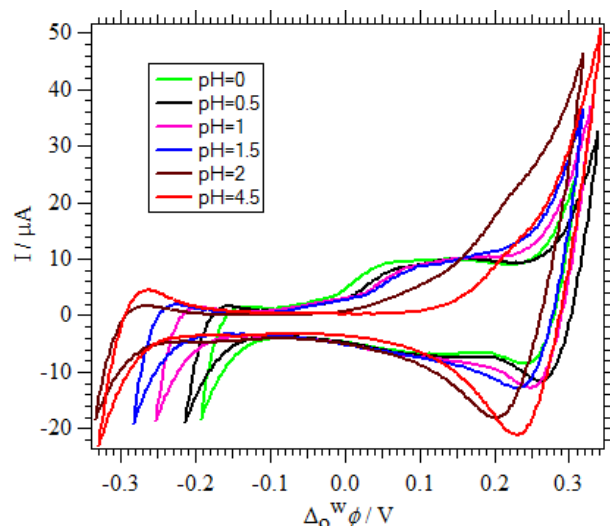


Figure 9. Cyclic voltammograms obtained by using electrochemical Cell 2 at different aqueous pH values. Scan rate was 50 mV/s.

addition, considering that charge values in the figures are associated with the desorbed protonated form of the phospholipid from the interface, the charge passing through the system also decreases as the pH increases (Figure 10b).

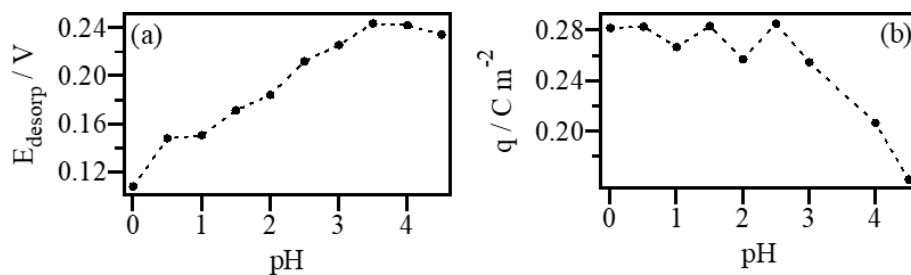


Figure 10. The plot of pH values of the aqueous phase vs. desorption potentials of the DPPC (a); the electrical charge passed on forward scan (b).

$$\Gamma = \frac{Q_{\max}}{zF} \quad (1)$$

In Eq. (1), Γ is surface excess concentration of phospholipid, Q_{\max} is the maximum surface charge density, z is charge, and F is Faraday's constant. Charge density is proportional to interfacial DPPC concentration. Accordingly, in the case that the charge passing through the system is known, the area per molecule can be calculated according to Eq. (1).³¹ Accordingly, this value (area per molecule) was found to be 58 \AA^2 . This result is in agreement with previous studies and suggests that the adsorption of DPPC at the interface is very high.^{8,10,13}

All of these results might be compatible with the mechanisms previously suggested for interactions between DPPC and H^+ .^{18,21,23} Thus, the zwitterionic phospholipid found in the organic phase is first adsorbed at the interface (1 of Figure 11).

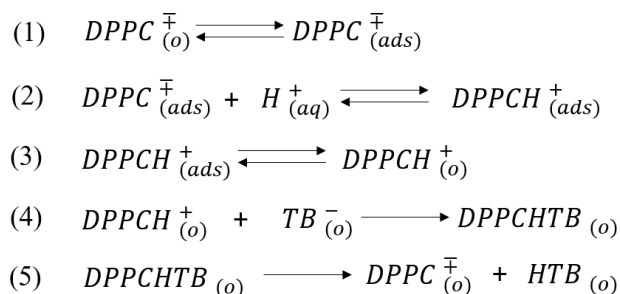


Figure 11. Possible mechanisms for DPPC/proton interaction at the ITIES.

Phospholipid molecules adsorbed at the interface then form an interfacial complex with the protons in the aqueous phase (2 of Figure 11). Thanks to mechanism 3 of Figure 11, the protonated form reaches an adsorption/desorption equilibrium. The validity of this mechanism might be explained by the fact that voltammetric signals shift toward lower potentials with increasing aqueous pH. This facilitates ion transfer of the proton (Figure 9). The phospholipid/proton complex reacts with the anion of the organic phase's supporting electrolyte in the organic phase (4 in Figure 11). Figure 3 can explain the validity of mechanism 4 in Figure 11.

Ionic form $DPPCH^+$ is adsorbed at the interface during the forward voltammetric scan. It then transfers into the organic phase, which is associated with the resulting current flow. If all of the phospholipid molecules adsorbed at the interface were transferred into the organic phase when the potential scan was reversed, then the potential would have become more negative. A current flow at the same density must have been observed. However, when the voltammogram is viewed, the backward peak current is lower than the forward peak current. This suggests that some phospholipid molecules stay at the interface. This suggests that the homogeneous reactions (mechanisms 4 and 5 of Figure 11) occur in the organic phase.

In conclusion, we describe the effects of both the pH of the aqueous phase and the concentration of the DPPC in the organic phase on the desorption of DPPC from a large water/DCE interface having an area of 1.52 cm^2 in a four-electrode cell. DPPC has strong interaction with the W/DCE interface. In addition, the adsorption of phospholipid at the interface depends on the pH of the aqueous phase, phospholipid concentration, and potential difference applied to the interface. This result agrees with results obtained from surface tension measurements.

3. Experimental

3.1. Reagents

Phospholipid DPPC (L- α -dipalmitoyl phosphatidylcholine), $M = 734.0 \text{ g/mol}$, was from Sigma (St. Louis, MO, USA). Hydrochloric acid (HCl, 32%) was from Merck (Darmstadt, Germany). The salt BATB (bis(triphenylphosphoranylidene) ammonium tetrakis(pentafluorophenyl) borate) was used as a supporting electrolyte in the organic phase. It was prepared by metathesis of BAcl (bis(triphenylphosphoranyldiene) ammonium chloride; Fluka, Buchs, Switzerland) and LiTB (lithium tetrakis(pentafluorophenyl) borate; Boulder Scientific, Mead, CO, USA). The salts BAcl and LiTB, dissolved in a 2:1 mixture of methanol:water, were gently mixed together and the resulting precipitate was filtered, washed thoroughly with water, and dried under vacuum. The salt was then further recrystallized in acetone. The crystals obtained were then dried under vacuum before use. The organic phase solvent used was DCE (1,2-DCE, 99%). Water (H_2O) was deionized by the Milli-Q water system (Bedford, MA, USA). The organic and aqueous solvents were mutually saturated prior to each experiment. All

the other solvents and reagents were of analytical grade and were employed without further purification, unless otherwise stated.

3.2. Preparation of the reference electrode

Reference electrode Ag/AgCl was prepared by connecting a newly polished silver wire and a platinum wire to the positive and negative terminals, respectively, of a battery with a voltage output of 1.5 V. An aqueous solution of NaCl plus a small amount of HCl plus a small amount of H₂SO₄ was employed as the electrolytic solution. The passage of current in the circuit produced a layer of insoluble silver salt on the silver wire, which was accompanied by the electrolytic reduction of proton at the platinum wire.

3.3. Electrochemical measurements

In voltammetric measurements at the ITIES, a programmable 4-electrode potentiostat (Autolab-PGSTAT 30, Metrohm, Herisau, Switzerland) and a homemade cubic cell made of borosilicate glass were used.^{32–35} The glass cell was cleaned using chromic acid, chloroform, and acetone and was rinsed thoroughly with ultrapure water. The interface was polarized by means of two reference electrodes (Ag/AgCl salt) and the current was collected via the two counter electrodes (Pt wires). The iR potential drop was compensated using a positive-feedback method.

Experimental potential refers directly to the chemical composition of the electrochemical cell and this potential scale is not appropriate to compare results from different experiments. Hence, CVs were plotted as a function of Galvani potential difference. This potential scale is determined experimentally by referencing each measurement with the transfer of tetramethylammonium cation (TEA⁺) at the interface. Formal potential of transfer of TEA⁺ at the interface has been taken equal to 0.160 V using an extrathermodynamic assumption.^{36,37} All of the measurements were carried out at room temperature of 22 ± 1 °C.

4. Acknowledgment

The Scientific and Technological Research Council of Turkey (TÜBİTAK, 2212) and the Scientific Research Projects Foundation of Selçuk University are gratefully acknowledged.

References

1. Peljo, P.; Girault, H. H. In *Encyclopedia of Analytical Chemistry*; Meyers, R. A., Ed. John Wiley & Sons: New York, NY, USA, 2012, pp. 1-28.
2. Reymond, F.; Fermin, D.; Lee, H. J.; Girault, H. H. *Electrochim. Acta* **2000**, *45*, 2647-2662.
3. Samec, Z. *Pure Appl. Chem.* **2004**, *76*, 2147-2180.
4. Molina, A.; Torralba, E.; Serna, C.; Ortuño, J. A. *Electrochim. Acta* **2013**, *106*, 244-257.
5. Kakiuchi, T.; Kondo, T.; Senda, M. *B. Chem. Soc. Jpn.* **1990**, *63*, 3270-3276.
6. Kakiuchi, T. In *Liquid-Liquid Interfaces. Theory and Methods*; Volkov, A. G.; Deamer, D. W., Eds. CRC Press: Boca Raton, FL, USA, 1996, pp. 317-331.
7. Murtomaki, L.; Manzanares, J. A.; Mafe, S.; Kontturi, K. In *Liquid Interfaces in Chemical, Biological and Pharmaceutical Applications*; Volkov, A. G., Ed. M. Dekker: New York, NY, USA, 2001, pp. 533-551.
8. Samec, Z.; Trojanek, A.; Krtil, P. *Faraday Discuss.* **2005**, *129*, 301-313.
9. Pichot, R.; Watson, R. L.; Norton I. T. *Int. J. Mol. Sci.* **2013**, *14*, 11767-11794.

10. Girault, H. H. J.; Schiffrin, D. J. *J. Electroanal. Chem.* **1984**, *179*, 277-284.
11. Girault, H. H.; Schiffrin, D. J. *Biochim. Biophys. Acta* **1986**, *857*, 251-258.
12. Samec, Z.; Trojáněk, A.; Girault, H. H. *Electrochem. Commun.* **2003**, *5*, 98-103.
13. Yoshida, Y.; Maeda, K.; Shirai, O. *J. Electroanal. Chem.* **2005**, *578*, 17-24.
14. Goto, T.; Maeda, K.; Yoshida, Y. *Langmuir* **2005**, *21*, 11788-11794.
15. Malkia, A.; Liljeroth, P.; Kontturi, K. *Electrochem. Commun.* **2003**, *5*, 473-479.
16. Chesniuk, S. G.; Dassie, S. A.; Yudi, L. M.; Baruzzi, A. M. *Electrochim. Acta* **1998**, *43*, 2175-2181.
17. Kakiuchi, T. *Electrochem. Commun.* **2000**, *2*, 317-321.
18. Jänchenová, H.; Lhotsky, A.; Stulík, K.; Marecek, V. *J. Electroanal. Chem.* **2007**, *601*, 101-106.
19. Jänchenová, H.; Stulík, K.; Marecek, V. *J. Electroanal. Chem.* **2007**, *604*, 109-114.
20. Jänchenová, H.; Stulík, K.; Marecek, V. *J. Electroanal. Chem.* **2008**, *612*, 186-190.
21. Holub, K.; Jänchenová, H.; Štulík, K.; Marecek, V. *J. Electroanal. Chem.* **2009**, *632*, 8-13.
22. Sovago, M.; Wurple, G. W. H.; Smits, M.; Muller, M.; Bonn, M. *J. Am. Chem. Soc.* **2007**, *129*, 11079-11084.
23. Mareček, V.; Lhotsky, A.; Jänchenová, H. *J. Phys. Chem. B* **2003**, *107*, 4573-4578.
24. Markin, V. S.; Volkov, A. G.; Volkova-Gugeshashvili, M. I. *J. Phys. Chem. B* **2005**, *109*, 16444-16454.
25. Méndez, M. A.; Su, B.; Girault, H. H. *J. Electroanal. Chem.* **2009**, *634*, 82-89.
26. Stockmann, T. J.; Noel, J. M.; Abou-Hassan, A.; Combellas, C.; Kanoufi, F. *J. Phys. Chem. C* **2016**, *120*, 11977-11983.
27. Vanýsek, P.; Ramírez, L. B. *J. Chil. Chem. Soc.* **2008**, *53*, 1455-1463.
28. Behr, B.; Gutknecht, J.; Schneider, H.; Stroka, J. *J. Electroanal. Chem.*, **1978**, *86*, 289-299.
29. Uyanik, I.; Cengeloglu, Y. *Electrochim. Acta* **2012**, *62*, 290-295.
30. Mendez, M. A.; Nazemi, Z.; Uyanik, I.; Lu, Y.; Girault, H. H. *Langmuir* **2011**, *27*, 13918-13924.
31. Mareček, V.; Lhotský, A.; Jänchenová, H. *J. Phys. Chem. B* **2003**, *107*, 4573-4578.
32. Mendez, M. A.; Prudent, M.; Su, B.; Girault, H. H. *Anal. Chem.* **2008**, *80*, 9499-9507.
33. Samec, Z.; Marecek, V.; Koryta, J.; Khalil, M. W. *J. Electroanal. Chem.* **1977**, *83*, 393-397.
34. Samec, Z.; Marecek, V.; Weber, J. *J. Electroanal. Chem.* **1979**, *103*, 11-18.
35. Samec, Z.; Marecek, V.; Weber, J. *J. Electroanal. Chem.* **1979**, *96*, 245-247.
36. Parker, A. J. *Electrochim. Acta* **1976**, *21*, 671-679.
37. Abraham, M. H.; De Namor, A. F. D. *J. Chem. Soc. Farad. T 1* **1976**, *72*, 955-962.